Shake before use: universal enhancement of quantum thermometry by unitary driving

Emanuele Tumbiolo ,^{1,2,*} Lorenzo Maccone ,^{1,2} Chiara Macchiavello ,^{1,2} Matteo G. A. Paris ,³ and Giacomo Guarnieri ,^{1,2}

Dipartimento di Fisica, Università degli Studi di Pavia, Via Agostino Bassi 6, I-27100, Pavia, Italy
 INFN Sezione di Pavia, Via Agostino Bassi 6, I-27100, Pavia, Italy
 Dipartimento di Fisica, Università di Milano, I- 20133, Milano, Italy

Quantum thermometry aims at determining temperature with ultimate precision in the quantum regime. Standard equilibrium approaches, limited by the Quantum Fisher Information given by static energy fluctuations, lose sensitivity outside a fixed temperature window. Non-equilibrium strategies have therefore been recently proposed to overcome these limits, but their advantages are typically model-dependent or tailored for a specific purpose. This Letter establishes a general, model-independent result showing that any temperature-dependent unitary driving applied to a thermalized probe enhances its quantum Fisher information with respect to its equilibrium value. Such information gain is expressed analytically through a positive semi-definite kernel of information currents that quantify the flow of statistical distinguishability. Our results are benchmarked on a driven spin-1/2 thermometer, furthermore showing that resonant modulations remarkably restore the quadratic-in-time scaling of the Fisher information and allow to shift the sensitivity peak across arbitrary temperature ranges. Our findings identify external unitary control as a universal resource for precision metrology and pave the way for future implementations in quantum sensing.

Introduction. – Unlike standard observables in quantum mechanics, temperature is notoriously not associated with a Hermitian operator and must be instead indirectly inferred [1-4]. In equilibrium quantum thermometry, a probe, hereby referred to as thermometer, is allowed to thermalize with a bath and the temperature is extracted from the statistics of energy measurements. According to quantum-estimation theory [5–7], the ultimate precision for any temperature estimation protocol is fixed by the quantum Fisher information (QFI) through the Cramér–Rao bound [8, 9]. For thermal states the QFI equals the thermometer's energy variance, and is thus proportional to its heat capacity [3, 10]. Yet equilibrium thermometry is fundamentally limited. Because Gibbs states commute with their Hamiltonian, the QFI coincides with the classical Fisher information of the thermal population distribution, with no contributions from coherence. Moreover, as we reach equilibrium, the QFI saturates and does not increase with the interrogation time. Last but not least, high sensitivity can be crucially achieved only within a fixed and non-tunable temperature window, dictated by the probe energy spectrum, and vanishes both in the low- and high-temperature limits [11, 12]. In practice, this hinders experimental control over the operating range of any equilibrium thermome-

These limitations have motivated the development of alternative, non-equilibrium approaches, such as interferometric [13–16] and control-assisted [17–19] schemes, where external drivings [20, 21] or transient dynamics [22–25] are exploited to enhance temperature sensitivity. Despite substantial progress, existing results remain largely model-dependent, and a unifying principle quantifying the fundamental role of unitary driving in quantum thermometry has insofar remained elusive. Here we

establish a universal, model-independent result: any unitary perturbation applied to a probe initially in thermal equilibrium cannot degrade its temperature sensitivity, and in fact enhances it under mild and physically reasonable assumptions. In particular, our main result is an analytical expression for the time-dependent QFI for a generic unitary driving, in the decomposed form

$$\mathcal{F}_t^{\beta} = \mathcal{F}_{\pi_0}^{\beta} + \mathcal{I}_t^{\beta}, \qquad \mathcal{I}_t^{\beta} \ge 0, \tag{1}$$

where $\mathcal{F}_{\pi_0}^{\beta}$ is the equilibrium value and \mathcal{I}_t^{β} quantifies the strictly non-negative contribution arising from the unitary driving. A general conclusion following from Eq. (1) is that any temperature-dependent unitary driving not only amplifies the general accuracy but also enables the shift-and-shape of the QFI profile across temperatures, effectively relocating the thermometer's high-sensitivity region to any desired range. This result holds for arbitrary finite-dimensional probes with full-rank initial states and can be naturally extended to more general settings. Although exemplified in the context of thermometry, our result extends directly to quantum estimation theory at large, providing a benchmark for precision enhancement in driven quantum systems.

Equilibrium thermometry. – In order to determine the temperature $(\beta^*)^{-1}$ of a target sample, acting as a thermal bath, the minimal strategy is to infer it from a probe (i.e. the thermometer) that has interacted with it until thermalization has occurred. Owing to the so-called "zero-th law" [26, 27] of Thermodynamics, such thermalization process in fact generally encodes the temperature β of a generic sample into the probe, leading to the definition of a smooth one-parameter statistical manifold $\{\pi_0(\beta)\}_{\beta}$, with $\pi_0(\beta) = e^{-\beta H_0}/Z_0$ being the Gibbs state of the probe with respect to its bare Hamiltonian H_0 . Within local quantum estimation theory, the max-

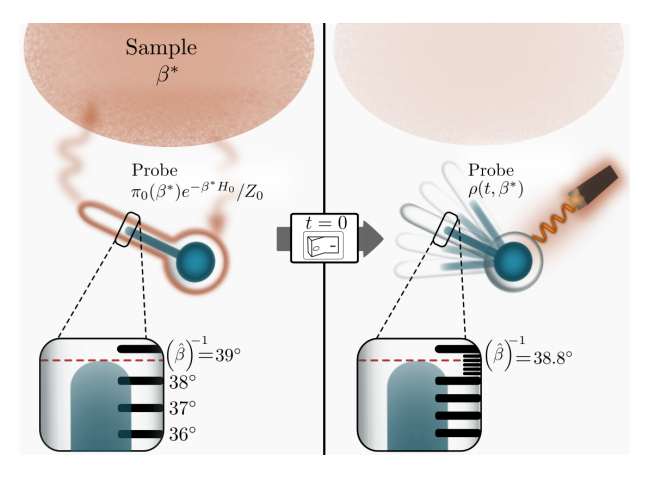


FIG. 1. Schematic illustration of the protocol. In the initial stage (left), the probe is allowed to thermalize with the sample, encoding the unknown inverse temperature β^* into the Gibbs state $\pi_0(\beta^*)$, and yielding an estimation precision bounded by the equilibrium quantum Cramér–Rao bound in Eq. (2). At t=0 the driving is switched on, perturbing the now isolated probe. The resulting QFI of the non-equilibrium state $\rho(t,\beta^*)$ evolves according to Eq. (1), increasing whenever the drive depends non-trivially on temperature and thereby enhancing the attainable precision in the estimation (here illustrated as the acquisition of an additional significant digit in the estimator $\hat{\beta}$).

imum achievable precision in inferring the true value of the parameter $\beta=\beta^*$ for any unbiased estimator $\hat{\beta}$ based on n independent measurements is set by the quantum Cramér-Rao bound

$$\operatorname{Var}[\hat{\beta}] \ge \frac{1}{n \mathcal{F}_{\pi_0}^{\beta^*}},\tag{2}$$

where $\mathcal{F}_{\pi_0}^{\beta^*} = \mathcal{F}_{\pi_0}^{\beta}|_{\beta=\beta^*}$ is the QFI, which represents the maximum of the classical Fisher information optimized over all positive operator-values measures, and quantifies the infinitesimal distinguishability between states in the statistical model. For an arbitrary smooth family of states $\sigma(\beta)$, the QFI can be explicitly expressed as

$$\mathcal{F}_{\sigma}^{\beta} = \operatorname{Tr}\left[(\partial_{\beta}\sigma)L_{\sigma}^{\beta}\right] = \operatorname{Tr}\left[\sigma\left(L_{\sigma}^{\beta}\right)^{2}\right],$$
 (3)

where the symmetric logarithmic derivative (SLD) [8] L^{β}_{σ} is the Hermitian operator satisfying the Lyapunov-type equation

$$\partial_{\beta}\sigma = \mathcal{J}_{\sigma}(L_{\sigma}^{\beta}), \qquad \mathcal{J}_{\sigma}(X) := \frac{1}{2}\{\sigma, X\}.$$
 (4)

The Bures-Jordan multiplication superoperator \mathcal{J}_{σ} [28, 29] induces a metric on the quantum statistical manifold parametrized by β through the inner product

$$\langle\!\langle A, B \rangle\!\rangle_{\sigma} = \operatorname{Tr} \left[A^{\dagger} \mathcal{J}_{\sigma}(B) \right].$$
 (5)

Accordingly, the SLD L^{β}_{σ} is the metric dual [30–32] of the tangent vector $\partial_{\beta}\sigma$, i.e. $L^{\beta}_{\sigma}=\mathcal{J}^{-1}_{\sigma}(\partial_{\beta}\sigma)$, where,

for full-rank σ , an explicit representation of the inverse Bures superoperator is $\mathcal{J}_{\sigma}^{-1}(X)=2\int_{0}^{\infty}ds\,e^{-s\sigma}\,X\,e^{-s\sigma}$. At thermal equilibrium, $[\pi_{0},H_{0}]=0$ implies

$$L_{\pi_0}^{\beta} = -(H_0 - \text{Tr}[H_0 \,\pi_0]), \tag{6}$$

$$\mathcal{F}_{\pi_0}^{\beta} = \operatorname{Var}_{\pi_0}[H_0], \tag{7}$$

which is proportional to the heat capacity of the probe up to a β^2 factor [33]. Because Eq. (2), with $\mathcal{F}_{\pi_0}^{\beta^*} = \mathcal{F}_{\pi_0}^{\beta}|_{\beta=\beta^*}$, is saturated by energy measurements, equilibrium thermometry is effectively classical and the achievable precision is fixed by static energy fluctuations. As the probe approaches π_0 , the QFI asymptotically saturates to Eq. (7), independently of the interrogation time t, in contrast with unitary metrological protocols where phase accumulation yields the characteristic quadratic scaling $\mathcal{F}_{\sigma}^{\beta} \propto t^2$ [34]. Moreover, the sensitivity window of equilibrium thermometry is static and determined by the spectrum of H_0 : for gapped systems the QFI is exponentially suppressed in both the $\beta \to 0$ (maximally mixed) and $\beta \to \infty$ (ground-state) limits, whereas for gapless ones it decays algebraically [3, 33]. These intrinsic limitations have motivated the exploration of non-equilibrium and control-assisted thermometric strategies, in which external drivings, engineered couplings [18, 35, 36], or memory effects [24, 25, 37] are exploited to activate coherence and modify the scaling and range of the QFI. A paradigmatic instance is that of periodically driven thermometers, where modulation of the probe spectrum can alter the low-temperature scaling of the achievable precision [21]. While such schemes demonstrate that control can outperform static thermometry, they remain tied to specific dynamics and platforms: a general, modelindependent understanding of how driving can reshape the fundamental bounds on thermal sensitivity is still lacking.

Driving a thermometer. — To single out the role of unitary control in determining temperature sensitivity, we consider the minimal scenario in which the probe, having first thermalized with the sample, is then subjected to an external perturbation mediated by a classical field, as depicted in Fig. 1. In this regime the dynamics is unitary, consistently with the standard formulation of quantum optimal control theory. The evolution is described by the propagator $U_{t,\beta}$, generated by the time-dependent Hamiltonian

$$H(t,\beta) = H_0 + \lambda(t,\beta)V, \tag{8}$$

where in general $[H_0,V] \neq 0$ and $\lambda(t,\beta)$ is a smooth driving profile in β . The temperature dependence of the drive encompasses the widest class of perturbations one can consider, and is motivated on both microscopic and operational grounds. From a thermodynamical perspective, the control field $\lambda(t,\beta)$ arises within an open quantum systems framework when the probe is coupled to an

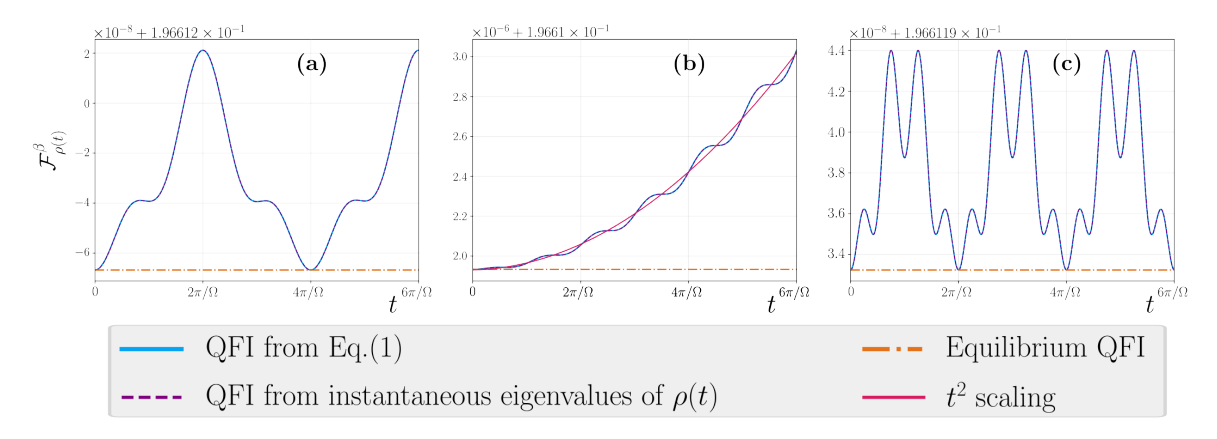


FIG. 2. Time evolution of the QFI for a single-spin probe under a temperature-dependent transverse driving. Time t is measured in units of the spin characteristic period $2\pi/\Omega$, with $\Omega=1$. Solid and dashed lines denote, respectively, the QFI as given by Eq. (1) and by the standard expression in terms of the instantaneous eigenvalues of $\rho(t)$ [38], showing perfect agreement. The dash-dotted line marks the equilibrium QFI benchmark. The three panels illustrate the transition from bounded dynamics to resonant quadratic scaling, identifying the optimal driving frequency. The Gaussian temperature control profile is chosen with a standard deviation saturating the equilibrium quantum Cramér–Rao bound, as if an optimal equilibrium estimation had been performed beforehand, and is randomly centered within the interval $\max\left(0, \beta^* \pm 1/\sqrt{\mathcal{F}_{\pi_0}^{\beta^*}}\right)$. For all panels $\phi=0$ and $\lambda_0=0.1$. (a) Off-resonant regime with $\omega_{\rm d}=0.5\,\Omega$, where the QFI exhibits bounded oscillations. (b) Resonant regime with $\omega_{\rm d}=\Omega$, where the QFI displays an almost monotonic t^2 growth, signalling a build-up of sensitivity. (c) High-frequency regime with $\omega_{\rm d}=2\,\Omega$, showing multi-frequency beating.

auxiliary work-reservoir, itself in equilibrium at the same temperature as the sample [39, 40].

In this regime, such a reservoir behaves in fact as an ideal work source with negligibly small fluctuations, unitarily exchanging energy with the probe and thus providing a deterministic, non-dissipative drive: tracing out its degrees of freedom yields an effective Hamiltonian correction on the probe whose amplitude inherits its β -dependence directly from the reservoir's thermal state [41, 42]. Operationally, one may engineer the driving profile in Eq. (8) adaptively, consistently with a local estimation framework: first of all, a preliminary coarsegrained measurement of the equilibrium probe provides a prior estimate $\beta_0 \approx \beta^*$ via Eq. (7), which is then used as a working point [43] to shape the control field and enhance the sensitivity in a neighborhood of β_0 . In the following, β_0, s_β are to be interpreted as fixed design parameters. In line with this perspective, and consistently with the thermodynamic interpretation above, in the rest of the paper we consider drivings of the form

$$\lambda(t,\beta) = \lambda_0 G_{\beta_0,s_\beta}(\beta) f(t), \tag{9}$$

where λ_0 is the driving strength, f(t) its temporal modulation, and $G_{\beta_0,s_\beta}(\beta) = \exp\left[-(\beta-\beta_0)^2/(2s_\beta^2)\right] \equiv G(\beta)$ a dimensionless Gaussian envelope centered around the initial estimate β_0 , with standard deviation s_β . This choice is purely illustrative and does not affect the generality of the protocol.

To assess how such drivings modify thermal sensitivity, we analyse the corresponding family of evolved states

 $\rho(t) = U_{t,\beta} \, \pi_0(\beta) \, U_{t,\beta}^{\dagger}$. Exploiting the unitary covariance of \mathcal{J}_{σ} and its inverse, the corresponding SLD can be expressed as

$$L_{\rho}^{\beta} = U_{t,\beta} \left(L_{\pi_{0}}^{\beta} + \delta L_{t}^{\beta} \right) U_{t,\beta}^{\dagger}, \tag{10}$$

with $L_{\pi_0}^{\beta}$ as in Eq. (6), while

$$\delta L_t^{\beta} = \int_0^t ds \, \partial_{\beta} \lambda(s) \, J_V(s) \tag{11}$$

captures the non-equilibrium contribution induced by the temperature dependence of the driving. The operator

$$J_V(s) = -\frac{i}{\hbar} \mathcal{J}_{\pi_0}^{-1}([V_H(s), \pi_0]), \qquad (12)$$

here introduced, which we call information current, quantifies the instantaneous flow of statistical distinguishability generated by the perturbation $V_H(s)$ (in the Heisenberg picture) with respect to the equilibrium reference state π_0 . It vanishes whenever $[V_H(s), \pi_0] = 0$, i.e. when no quantum friction is generated through the driving, since the latter leaves the eigenbasis of π_0 invariant, acting only on its eigenvalues [44–48]. Hence, a nonzero $J_V(s)$ signals that the control field injects coherences in the eigenbasis of π_0 : the ensuing enhancement of distinguishability thus stems from a genuinely quantum mechanism. Similarly, when $\partial_\beta \lambda = 0$, i.e. when the driving is not sensitive to temperature, one recovers $L_{\rho(t)}^\beta = L_{\pi_0}^\beta$. This identifies a genuine no-go condition, as it excludes any unitary control that does not explicitly depend on

 β from generating additional information about temperature, regardless of its time dependence or strength. Geometrically, this reflects the fact that a parameter-independent unitary is an isometry of the Bures metric, rotating the probe state within the statistical manifold without changing its sensitivity to temperature. This conclusion is fully consistent with the quantum data-processing inequality [49], which forbids any Fisher information gain under parameter-independent completely positive trace-preserving maps, including unitaries.

Using Eq. (3) and noticing that $\text{Tr}\left[\pi_0 \,\delta L_t^\beta \,L_{\pi_0}^\beta\right] = 0$, allows to derive [50] our main result Eq. (1), which quantifies the QFI increment due to a generic unitary driving with

$$\mathcal{I}_{t}^{\beta} = \operatorname{Tr}\left[\pi_{0}(\beta) \left(\delta L_{t}^{\beta}\right)^{2}\right] = \\
= \int_{0}^{t} \int_{0}^{t} \partial_{\beta} \lambda(s,\beta) \,\partial_{\beta} \lambda(u,\beta) \,K(s,u,\beta) \,ds \,du \,. \tag{13}$$

which is manifestly non-negative, and where we have introduced the kernel

$$K(s, u, \beta) = \text{Tr}[\pi_0(\beta) J_V(s) J_V(u)]$$
 (14)

which encodes the two-time correlation function of the information current. We remark once again that the QFI has to be evaluated at $\beta = \beta^*$ and that, if the perturbation commutes with the initial Hamiltonian, i.e. $[H_0, V] = 0$, then the improvement vanishes and no precision enhancement is expected.

Interestingly, by interpreting the external driving as part of a measurement scheme, our results can be recast within the framework of quantum parameter estimation with parameter-dependent measurement apparatuses, put forward in Ref. [51], where the standard Cramér-Rao bound may in principle be surpassed. In the present work, however, we focus explicitly on the modification of the QFI induced by the β -dependent dynamics, without optimizing the drive. In this sense, Eq. (1) holds true for any arbitrary choice of driving provided it depends non-trivially on temperature.

The positivity of Eq. (13) thus provides a universal measure of how temperature-dependent drivings amplify thermal sensitivity. At short times, regularity of the kernel guarantees that $\mathcal{I}_t^{\beta} \sim t^2$, reproducing the standard scaling of the QFI in closed evolutions where distinguishability grows linearly in time at the level of the SLD. Importantly, the same quadratic scaling can re-emerge asymptotically when the driving preserves constructive correlations in the information current, such as for constant controls or for periodic modulations resonant with the Bohr frequencies of H_0 . This guarantees the scaling of the QFI with t to be quantum-like, i.e. quadratic, at all times [34]. Since the kernel depends on the β -derivative of the control profile $\lambda(t,\beta)$, shaping this dependence provides a direct way of shifting the sensitivity window of the

probe. In this sense, the driving acts as an operational handle on the probe sensitivity landscape, and can naturally accommodate feedback-assisted strategies in which $\lambda(t,\beta)$ is updated in real time according to intermediate estimates of β , keeping the probe dynamically locked to the region of maximal information gain. To benchmark these general results, we analyze a single spin probe as a minimal reference model in which all relevant mechanisms can be made explicit.

Single spin probe. – In this minimal setting, the dynamics is governed by a driven two-level Hamiltonian,

$$H(t,\beta) = \frac{\Omega}{2}\sigma_z + \lambda(t,\beta)\sigma_x, \tag{15}$$

where Ω denotes the characteristic frequency of the system, while $\lambda(t,\beta)$ is chosen according to Eq. (9), with periodic temporal modulation, $f(t) = \cos(\omega_{\rm d} t + \phi)$, driving frequency $\omega_{\rm d}$ and phase ϕ . In the absence of control, the probe is allowed to reach thermal equilibrium, characterized by the baseline Fisher information

$$\mathcal{F}_{\pi_0}^{\beta} = \left(\frac{\Omega}{2}\right)^2 \operatorname{sech}^2\left(\frac{\beta\Omega}{2}\right). \tag{16}$$

Switching on the drive turns on the information current, leading to the emergence of a non-trivial $K(s, u, \beta)$.

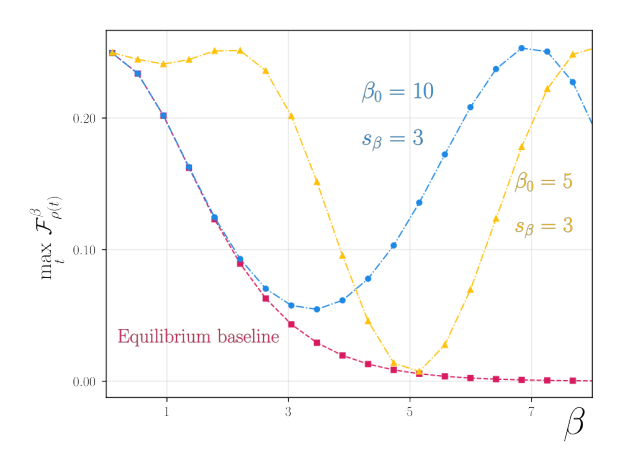


FIG. 3. Behaviour of the maximum QFI at a fixed evolution time $t=12\,s$ in the resonant regime, as a function of the inverse temperature β . The magenta dashed line (with squares) represents the equilibrium baseline $\mathcal{F}_{\pi_0}^{\beta}$, while the blue circles and yellow triangles show the maxima for the driven case, for $G(\beta)$ with $(\beta_0, s_\beta) = (10, 3)$ and (5, 3), respectively. By tuning the mean and standard deviation of the Gaussian envelope, the sensitivity window can be shifted to different temperature ranges. The resulting QFI profiles display two symmetric lobes around β_0 , reflecting the underlying Gaussian modulation of the driving amplitude, as exemplified by the yellow curve.

The time integral governing \mathcal{I}_t^{β} contains harmonic components oscillating at $\Omega \pm \omega_d$, with the detuning $\Omega - \omega_d$ determining whether correlations in the information current interfere constructively or destructively over

time. Fig. 2 illustrates this effect for three representative driving frequencies: below, on, and above resonance. On resonance, i.e. $\omega_{\rm d} \simeq \Omega$, and in a weak-field approximation,

the increment \mathcal{I}_t^{β} can be shown explicitly [50] to achieve quadratic scaling for long times

$$\mathcal{I}_t^{\beta} \approx \left(\lambda_0 G'(\beta)\right)^2 \alpha(\beta) t^2 \,, \tag{17}$$

with $G'(\beta) = \partial_{\beta}G(\beta)$ and $\alpha(\beta)$ being a time-independent quantity dictated only by the equilibrium state of the thermometer, confirming that resonance restores the fully unitary t^2 scaling discussed above. For detuned drivings ($\omega_d \neq \Omega$), instead, the oscillatory kernel induces dephasing that suppresses the long-time growth and saturates the information gain.

In Fig. 3, we fix $\omega_{\rm d} \simeq \Omega$ and vary the center and standard deviation of the Gaussian temperature envelope, showing how the QFI can be reshaped and shifted across distinct temperature regions. This demonstrates that the probe's sensitivity window can be tailored on demand by engineering the functional dependence of the control amplitude on β .

Conclusion. – In this work we have derived a universal analytic expression for the temperature sensitivity, i.e. its Quantum Fisher Information, ensuing from a general temperature-dependent unitary driving of an initially thermalized probe. Our results show that implementing such a perturbation always increases temperature precision, quantified by a non-negative correction to the equilibrium heat capacity of the thermometer expressed in terms of a positive kernel of information-geometric currents that quantifies the unitary build-up of temperature information along the unitary drive. We then showcase our findings on a driven spin-1/2 model, remarkably recovering a t^2 scaling of the QFI in the resonantdriving regime. Furthermore, we explicitly demonstrate that the sensitivity window of the qubit probe can be tuned across the whole temperature range by suitably acting on the driving parameters. We want to emphasize that the framework and the results here explicitly obtained within the context of quantum thermometry can be straightforwardly applied to study the enhancement of other parameters estimation. Finally, it is worth mentioning that the predicted sensitivity enhancement and tunability can be directly applicable to current experimental setups for quantum thermometry such as bichromatically driven trapped ions [52] or microwave-driven dispersive circuit QED [53-55]. A natural next step will be to allow for the control field to act already during thermalization, or to consider non-unitary drivings, thus allowing to characterize the tradeoff between coherent control and dissipation in thermal sensitivity enhancements.

ACKNOWLEDGMENTS

E.T. acknowledges support from the PNRR MUR Project PE0000023-NQSTI. G.G. kindly acknowledges support from the Ministero dell'Università e della Ricerca (MUR) under the "Rita Levi-Montalcini" grant and to INFN. L.M. acknowledges support from the PRIN MUR Project 2022RATBS4. C.M. acknowledges support from the National Research Centre for HPC, Big Data and Quantum Computing, PNRR MUR Project CN0000013-ICSC. M.G.A.P acknowledges partial support by Khalifa University of Science and Technology through the project C2PS-8474000137.

- * Corresponing author: emanuele.tumbiolo01@ateneopv.it
- [1] J. Gemmer, M. Michel, and G. Mahler, Quantum Thermodynamics: Emergence of Thermodynamic Behavior Within Composite Quantum Systems, Lecture Notes in Physics, Vol. 784 (Springer, 2009).
- [2] A. Puglisi, A. Sarracino, and A. Vulpiani, Temperature in and out of equilibrium: A review of concepts, tools and attempts, Physics Reports **709-710**, 1 (2017).
- [3] M. Mehboudi, A. Sanpera, and L. A. Correa, Thermometry in the quantum regime: recent theoretical progress, Journal of Physics A: Mathematical and Theoretical 52, 303001 (2019).
- [4] M. Jørgensen, *Ultimate precision bounds on quantum thermometry*, Ph.D. thesis, Department of Physics, Technical University of Denmark (2021).
- [5] C. W. Helstrom, Quantum Detection and Estimation Theory, Mathematics in Science and Engineering, Vol. 123 (Academic Press, New York, 1976).
- [6] V. Giovannetti, S. Lloyd, and L. Maccone, Quantumenhanced measurements: Beating the standard quantum limit, Science 306, 1330 (2004).
- [7] V. Giovannetti, S. Lloyd, and L. Maccone, Quantum metrology, Physical Review Letters 96, 010401 (2006).
- [8] M. G. A. Paris, Quantum estimation for quantum technology, International Journal of Quantum Information 07, 125 (2009).
- [9] S. L. Braunstein and C. M. Caves, Statistical distance and the geometry of quantum states, Physical Review Letters 72, 3439 (1994).
- [10] L. A. Correa, M. Mehboudi, G. Adesso, and A. Sanpera, Individual quantum probes for optimal thermometry, Phys. Rev. Lett. 114, 220405 (2015).
- [11] P. P. Potts, J. B. Brask, and N. Brunner, Fundamental limits on low-temperature quantum thermometry with finite resolution, Quantum 3, 161 (2019).
- [12] M. R. Jørgensen, P. P. Potts, M. G. A. Paris, and J. B. Brask, Tight bound on finite-resolution quantum thermometry at low temperatures, Physical Review Research 2, 033394 (2020).

- [13] A. De Pasquale and T. M. Stace, Quantum thermometry, in *Thermodynamics in the Quantum Regime: Fundamental Aspects and New Directions*, edited by F. Binder, L. A. Correa, C. Gogolin, J. Anders, and G. Adesso (Springer International Publishing, 2018) pp. 503–527.
- [14] M. Jarzyna and M. Zwierz, Quantum interferometric measurements of temperature, Phys. Rev. A 92, 032112 (2015).
- [15] H. Yang, Q. Zheng, P. Yue, and Q. Zhi, Quantum thermometry based on interferometric power, Europhysics Letters 146, 38002 (2024).
- [16] D. Y. Akamatsu, L. F. R. de Moura, G. G. Damas, G. D. de Moraes Neto, V. Montenegro, and N. G. de Almeida, Probing the limits of dispersive quantum thermometry with a nonlinear mach-zehnder-based quantum simulator (2025), arXiv:2507.04246.
- [17] M. Mehboudi, M. R. Jørgensen, S. Seah, J. B. Brask, J. Kołodyński, and M. Perarnau-Llobet, Fundamental limits in bayesian thermometry and attainability via adaptive strategies, Phys. Rev. Lett. 128, 130502 (2022).
- [18] A. H. Kiilerich, A. De Pasquale, and V. Giovannetti, Dynamical approach to ancilla-assisted quantum thermometry, Phys. Rev. A 98, 042124 (2018).
- [19] P. Sekatski and M. Perarnau-Llobet, Optimal nonequilibrium thermometry in Markovian environments, Quantum 6, 869 (2022).
- [20] V. Mukherjee, A. Zwick, A. G. Kofman, and G. Kurizki, Enhanced low-temperature thermometry by external control, Communications Physics 2, 162 (2019).
- [21] J. Glatthard and L. A. Correa, Bending the rules of low-temperature thermometry with periodic driving, Quantum 6, 705 (2022).
- [22] S. Razavian, C. Benedetti, M. Bina, Y. Akbari-Kourbolagh, and M. G. Paris, Quantum thermometry by single-qubit dephasing, The European Physical Journal Plus 134, 284 (2019).
- [23] F. Gebbia, C. Benedetti, F. Benatti, R. Floreanini, M. Bina, and M. G. A. Paris, Two-qubit quantum probes for the temperature of an ohmic environment, Phys. Rev. A 101, 032112 (2020).
- [24] N. Zhang, C. Chen, and P. Wang, Enhancing low-temperature quantum thermometry via sequential measurements, Phys. Rev. Appl. 24, 044008 (2025).
- [25] Y. Yang, V. Montenegro, and A. Bayat, Sequential-measurement thermometry with quantum many-body probes, Phys. Rev. Appl. 22, 024069 (2024).
- [26] M. Planck, Treatise on Thermodynamics (Dover Publications, New York, 1990) originally published in German in 1897.
- [27] H. B. Callen, Thermodynamics and an Introduction to Thermostatistics, 2nd ed. (Wiley, New York, 1985).
- [28] M. Scandi, H. J. D. Miller, J. Anders, and M. Perarnau-Llobet, Quantum work statistics close to equilibrium, Phys. Rev. Res. 2, 023377 (2020).
- [29] P. Abiuso, P. Sekatski, J. Calsamiglia, and M. Perarnau-Llobet, Fundamental limits of metrology at thermal equilibrium, Phys. Rev. Lett. 134, 010801 (2025).
- [30] F. M. Ciaglia, J. Jost, and L. J. Schwachhöfer, Differential geometric aspects of parametric estimation theory for states on finite-dimensional c*-algebras, Entropy 22, 1332 (2020).
- [31] D. Petz, Quantum Information Theory and Quantum Statistics, Theoretical and Mathematical Physics (Springer, Berlin, Heidelberg, 2008).

- [32] S. ichi Amari and H. Nagaoka, Methods of Information Geometry, Translations of Mathematical Monographs, Vol. 191 (American Mathematical Society, Providence, RI, 2000).
- [33] M. G. A. Paris, Achieving the landau bound to precision of quantum thermometry in systems with vanishing gap, Journal of Physics A: Mathematical and Theoretical 49, 03LT02 (2015).
- [34] A. Das, W. Górecki, and R. Demkowicz-Dobrzański, Universal time scalings of sensitivity in markovian quantum metrology, Phys. Rev. A 111, L020403 (2025).
- [35] G. Planella, M. F. B. Cenni, A. Acín, and M. Mehboudi, Bath-induced correlations enhance thermometry precision at low temperatures, Physical Review Letters 128, 040502 (2022).
- [36] P. Abiuso, P. Andrea Erdman, M. Ronen, F. Noé, G. Haack, and M. Perarnau-Llobet, Optimal thermometers with spin networks, Quantum Science and Technology 9, 035008 (2024).
- [37] Y. Aiache, C. Seida, K. El Anouz, and A. El Allati, Non-markovian enhancement of nonequilibrium quantum thermometry, Phys. Rev. E 110, 024132 (2024).
- [38] J. Liu, H. Yuan, X.-M. Lu, and X. Wang, Quantum fisher information matrix and multiparameter estimation, Journal of Physics A: Mathematical and Theoretical 53, 023001 (2019).
- [39] A. Colla and H.-P. Breuer, Thermodynamic roles of quantum environments: from heat baths to work reservoirs, Quantum Science and Technology 10, 015047 (2024).
- [40] P. Strasberg, Quantum Stochastic Thermodynamics: Foundations and Selected Applications, Oxford Graduate Texts (Oxford University Press, Oxford, UK, 2022).
- [41] M. Campisi, P. Talkner, and P. Hänggi, Fluctuation theorem for arbitrary open quantum systems, Phys. Rev. Lett. 102, 210401 (2009).
- [42] A. S. Trushechkin, M. Merkli, J. D. Cresser, and J. Anders, Open quantum system dynamics and the mean force gibbs state, AVS Quantum Science 4 (2022).
- [43] V. Giovannetti, S. Lloyd, and L. Maccone, Advances in quantum metrology, Nature Photonics 5, 222 (2011).
- [44] T. Feldmann and R. Kosloff, Quantum four-stroke heat engine: Thermodynamic observables in a model with intrinsic friction, Phys. Rev. E 68, 016101 (2003).
- [45] F. Plastina, A. Alecce, T. J. G. Apollaro, G. Falcone, G. Francica, F. Galve, N. Lo Gullo, and R. Zambrini, Irreversible work and inner friction in quantum thermodynamic processes, Phys. Rev. Lett. 113, 260601 (2014).
- [46] H. J. D. Miller, M. H. Mohammady, M. Perarnau-Llobet, and G. Guarnieri, Thermodynamic uncertainty relation in slowly driven quantum heat engines, Phys. Rev. Lett. 126, 210603 (2021).
- [47] O. Onishchenko, G. Guarnieri, P. Rosillo-Rodes, D. Pijn, J. Hilder, U. G. Poschinger, M. Perarnau-Llobet, J. Eisert, and F. Schmidt-Kaler, Probing coherent quantum thermodynamics using a trapped ion, Nature Communications 15, 6974 (2024).
- [48] G. Francica, J. Goold, and F. Plastina, Role of coherence in the nonequilibrium thermodynamics of quantum systems, Phys. Rev. E 99, 042105 (2019).
- [49] D. Petz, Monotone metrics on matrix spaces, Linear Algebra and its Applications 244, 81 (1996).
- [50] See supplemental material.
- [51] L. Seveso, M. A. C. Rossi, and M. G. A. Paris, Quantum metrology beyond the quantum cramér-rao theorem,

Phys. Rev. A 95, 012111 (2017).

- [52] X.-Q. Li, Y. Tao, T. Chen, W. Wu, Y. Xie, C.-W. Wu, and P.-X. Chen, Thermometry of trapped ions based on bichromatic driving, Phys. Rev. Appl. 22, 064022 (2024).
- [53] J. Gambetta, A. Blais, D. I. Schuster, A. Wallraff, L. Frunzio, J. Majer, M. H. Devoret, S. M. Girvin, and R. J. Schoelkopf, Qubit-photon interactions in a cavity: Measurement-induced dephasing and number splitting, Phys. Rev. A 74, 042318 (2006).
- [54] A. P. Sears, A. Petrenko, G. Catelani, L. Sun, H. Paik, G. Kirchmair, L. Frunzio, L. I. Glazman, and R. J. Schoelkopf, Photon shot noise dephasing in the strongdispersive limit of circuit qed, Phys. Rev. B 86, 180504

(2012).

- [55] J. Atalaya, A. Opremcak, A. Nersisyan, K. Lee, and A. N. Korotkov, Measurement of small photon numbers in circuit qed resonators, Phys. Rev. Lett. 132, 203601 (2024).
- [56] D. Petz and C. Sudár, Geometries of quantum states, Journal of Mathematical Physics 37, 2662 (1996).
- [57] E. A. Morozova and N. N. Čencov, Markov invariant geometry on state manifolds, in *Current Problems in Mathematics*. Newest Results, Vol. 36 (VINITI, Moscow, 1989) pp. 69–102, in Russian.
- [58] M. Scandi, Information and Thermodynamics, Ph.D. thesis, Institut de Ciències Fotòniques (ICFO), Universitat Politècnica de Catalunya (2023).

Supplemental Material

S1: DERIVING THE EXPRESSION FOR THE DYNAMICAL INCREMENT OF THE QFI

In this section we derive the two central identities of this work, namely Eqs. (1) and (13) of the main text. The former expresses the quantum Fisher information of the driven probe at time t as

$$\mathcal{F}_{\rho(t)}^{\beta} = \mathcal{F}_{\pi_0}^{\beta} + \mathcal{I}_t^{\beta},\tag{S1}$$

i.e. as the sum of an equilibrium baseline, fixed by the initial thermal state, and a purely dynamical, non-negative increment \mathcal{I}_t^{β} generated by the drive. Equation (13), instead, provides an exact closed form for such an increment.

To set the stage, we recall the standard geometric interpretation of the QFI as a quantifier of local sensitivity in quantum parameter estimation. Since we are concerned with thermometry, we restrict to the one-parameter scenario of the inverse temperature β , but all considerations extend to the multiparameter case.

Consider a finite-dimensional thermometer with Hilbert space \mathcal{H} and a smooth, one-parameter family of full-rank density operators $\{\sigma(\beta)\}$. The mapping $\beta \mapsto \sigma(\beta)$ defines a statistical manifold whose tangent space at each point σ consists of traceless Hermitian operators and is spanned by the derivative vector $\partial_{\beta}\sigma$.

Such a manifold is Riemannian upon the choice of a suitable metric $g_{\sigma}(X,Y)$ for X,Y in the tangent space at σ . According to the Morozova-Čencov-Petz classification, the admissible metrics form a continuous family generated by operator-monotone functions. We refer the reader to [49, 56–58] for further information. In quantum parameter estimation, the canonical and operationally relevant choice is the Bures metric, induced by the Bures inner product

$$\langle\!\langle X, Y \rangle\!\rangle_{\sigma} = \text{Tr}[X^{\dagger} \mathcal{J}_{\sigma}(Y)],$$
 (S2)

where $\mathcal{J}_{\sigma}(Y) = \frac{1}{2} \{\sigma, Y\}$ is the Bures–Jordan superoperator with inverse

$$\mathcal{J}_{\sigma}^{-1}(X) = 2 \int_0^\infty e^{-s\sigma} X e^{-s\sigma} ds.$$
 (S3)

Both are unitarily covariant: for an arbitrary unitary U,

$$\mathcal{J}_{U\sigma U^{\dagger}}(X) = U \,\mathcal{J}_{\sigma}(U^{\dagger}XU) \,U^{\dagger}, \qquad \mathcal{J}_{U\sigma U^{\dagger}}^{-1}(X) = U \,\mathcal{J}_{\sigma}^{-1}(U^{\dagger}XU) \,U^{\dagger}, \tag{S4}$$

a property that will be needed further in the derivation. Within this structure

$$g_{\sigma}^{(B)}(\partial_{\beta}\sigma, \partial_{\beta}\sigma) = \langle \langle \mathcal{J}_{\sigma}^{-1}(\partial_{\beta}\sigma), \mathcal{J}_{\sigma}^{-1}(\partial_{\beta}\sigma) \rangle \rangle_{\sigma} = \text{Tr} \left[\partial_{\beta}\sigma \, \mathcal{J}_{\sigma}^{-1}(\partial_{\beta}\sigma) \right]. \tag{S5}$$

By identifying the dual under this metric of the tangent vector $\partial_{\beta}\sigma$ as the symmetric logarithmic derivative (SLD),

$$L_{\sigma}^{\beta} := \mathcal{J}_{\sigma}^{-1}(\partial_{\beta}\sigma), \tag{S6}$$

i.e. the unique solution to the Lyapunov-type equation $\partial_{\beta}\sigma = \frac{1}{2}\{\sigma, L_{\sigma}^{\beta}\}$, it is immediate to show that

$$g_{\sigma}^{(B)} = \frac{1}{4} \operatorname{Tr} \left[\sigma \left(L_{\sigma}^{\beta} \right)^{2} \right], \tag{S7}$$

where the right-hand side is exactly one quarter of the standard QFI, i.e.

$$\mathcal{F}_{\sigma}^{\beta} = \text{Tr}\left[\sigma \left(L_{\sigma}^{\beta}\right)^{2}\right]. \tag{S8}$$

Hence, the QFI $\mathcal{F}^{\beta}_{\sigma}$ appears naturally as the local Bures metric (up to a multiplicative factor) of the statistical model, representing the squared infinitesimal distance between neighbouring states $\sigma(\beta)$ and $\sigma(\beta + d\beta)$ and thus quantifying the distinguishability of nearby states and the sensitivity of the model to changes in the parameter β .

With this in mind and in order to assess the effect of unitary driving on local distinguishability, our goal is to compute the QFI of $\rho(t, \beta)$ according to Eq. (S8).

We recall the main assumptions concerning the dynamics under consideration:

- 1. At time t=0, the state of the thermometer is thermal (at inverse temperature β) with respect to its bare Hamiltonian, as a result of thermalization with a sample (whose temperature we want to estimate) that has then been subsequently disconnected from the probe. Thus, the initial manifold is that of Gibbs states $\{\pi_0(\beta)\}$, equipped with QFI $\mathcal{F}_{\pi_0}^{\beta} = \operatorname{Var}_{\pi_0}(H_0)$.
- 2. At times t > 0, the probe Hamiltonian is coupled to an external perturbation V, yielding $H(t, \beta) = H_0 + \lambda(t, \beta)V$, with $\lambda(t, \beta)$ the driving profile, assumed to be temperature-dependent in the most general setting. The ensuing dynamics is $\rho(t, \beta) = U_{t,\beta}\pi_0(\beta)U_{t,\beta}^{\dagger}$, with $U_{t,\beta} = \mathcal{T}\exp\left[-\frac{i}{\hbar}\int_0^t H(s, \beta)\,ds\right]$.

First, notice that, exploiting the unitary covariance of $\mathcal{J}_{\rho(t)}$ and its inverse, one can compute the SLD at time t, appearing in the definition of the QFI, from its expression at the reference state π_0 .

Differentiating $\rho(t,\beta)$ with respect to β yields

$$\partial_{\beta}\rho(t,\beta) = U_{t,\beta} \Big(\partial_{\beta}\pi_0 + [A(t,\beta), \,\pi_0] \Big) U_{t,\beta}^{\dagger}, \qquad A(t,\beta) := U_{t,\beta}^{\dagger} \,\partial_{\beta}U_{t,\beta}, \tag{S9}$$

which separates the equilibrium derivative $\partial_{\beta}\pi_0$ from the dynamical contribution generated by $A(t,\beta)$. Then, from Eq. (S4),

$$L_{\rho(t)}^{\beta} = U_{t,\beta} \left[\mathcal{J}_{\pi_0}^{-1}(\partial_{\beta}\pi_0) + \mathcal{J}_{\pi_0}^{-1}([A(t,\beta),\pi_0]) \right] U_{t,\beta}^{\dagger}, \tag{S10}$$

or equivalently

$$L_{\rho(t)}^{\beta} = U_{t,\beta} \left(L_{\pi_0}^{\beta} + \delta L_t^{\beta} \right) U_{t,\beta}^{\dagger}, \tag{S11}$$

having distinguished the equilibrium baseline $L_{\pi_0}^{\beta} = -(H_0 - \text{Tr}[\pi_0(\beta)H_0])$ from the dynamical correction δL_t^{β} . We thus need to compute the explicit form of $A(t,\beta)$, which requires differentiating $U_{t,\beta}$. The Dyson expansion of the unitary propagator reads

$$U_{t,\beta} = U(t,0;\beta) = 1 + \sum_{n=1}^{\infty} \left(-\frac{i}{\hbar}\right)^n \int_{0 < t_1 < \dots < t_n < t} dt_1 \cdots dt_n \ H(t_n,\beta) \cdots H(t_1,\beta), \tag{S12}$$

where t_n is the latest and t_1 the earliest time variable. Differentiating each term of Eq. (S12) with respect to β gives

$$\partial_{\beta}U(t,0;\beta) = \sum_{n=1}^{\infty} \left(-\frac{i}{\hbar}\right)^{n} \int_{0 < t_{1} < \dots < t_{n} < t} dt_{1} \dots dt_{n} \sum_{k=1}^{n} \left[\left(\prod_{r=k+1}^{n} H(t_{r},\beta)\right) (\partial_{\beta}H(t_{k},\beta)) \left(\prod_{r=1}^{k-1} H(t_{r},\beta)\right) \right], \tag{S13}$$

with the convention

$$\prod_{r=a}^{b} X_r := 1 \qquad \text{whenever } a > b, \tag{S14}$$

so that the terms k = 1 and k = n are automatically included.

For a fixed k, we set $s := t_k$ and split the integration variables into the subsets $\{t_j > s\}$ and $\{t_j < s\}$. Recognizing the corresponding partial propagators,

$$U(t,s;\beta) = 1 + \sum_{p=1}^{\infty} \left(-\frac{i}{\hbar} \right)^p \int_{s < t_{k+1} < \dots < t_n < t} dt_{k+1} \dots dt_n \prod_{r=k+1}^n H(t_r,\beta),$$

$$U(s,0;\beta) = 1 + \sum_{q=1}^{\infty} \left(-\frac{i}{\hbar} \right)^q \int_{0 < t_1 < \dots < t_{k-1} < s} dt_1 \dots dt_{k-1} \prod_{r=1}^{k-1} H(t_r,\beta),$$
(S15)

and summing over k we recover

$$\partial_{\beta}U(t,0;\beta) = -\frac{i}{\hbar} \int_{0}^{t} U(t,0;\beta) U^{\dagger}(s,0;\beta) \,\partial_{\beta}H(s,\beta) U(s,0;\beta) \,ds. \tag{S16}$$

Right-multiplying Eq. (S16) by $U^{\dagger}(t,0,\beta)$ then yields

$$A(t,\beta) = -\frac{i}{\hbar} \int_0^t U^{\dagger}(s,\beta) \left(\partial_{\beta} H(s,\beta)\right) U(s,\beta) ds = -\frac{i}{\hbar} \int_0^t U_{s,\beta}^{\dagger} \left(\partial_{\beta} H(s,\beta)\right) U_{s,\beta} ds. \tag{S17}$$

For our additive driving, $\partial_{\beta}H(t,\beta) = \partial_{\beta}\lambda(t,\beta)V$, which gives

$$A(t,\beta) = -\frac{i}{\hbar} \int_0^t (\partial_\beta \lambda(s,\beta)) V_H(s) ds, \tag{S18}$$

where $V_H(s) := U^{\dagger}(s,\beta) V U(s,\beta)$ is the Heisenberg-picture time-evolved perturbation. Substituting Eq. (S18) into Eq. (S11) and using the linearity of $\mathcal{J}_{\pi_0}^{-1}$ gives

$$\delta L_t^{\beta} = \int_0^t (\partial_{\beta} \lambda(s, \beta)) J_V(s) ds, \tag{S19}$$

having defined the information current operator

$$J_V(s) := -\frac{i}{\hbar} \mathcal{J}_{\pi_0}^{-1}([V_H(s), \pi_0]). \tag{S20}$$

Notice that, if $[V_H(s), \pi_0] = 0$ at all times, then $J_V(s) = 0$ and hence $\delta L_t^{\beta} = 0$: no dynamical correction to the SLD arises, and the QFI remains frozen at its equilibrium value. Consistently, in the eigenbasis of π_0 , the commutator $[V_H(s), \pi_0]$ has only off-diagonal matrix elements, and the inverse superoperator $\mathcal{J}_{\pi_0}^{-1}$ preserves this structure. Therefore $J_V(s)$ acts entirely within the operator subspace orthogonal to $\pi_0(\beta)$, i.e. it is associated with the generation of coherences in the energy eigenbasis of the thermal state.

Combining Eqs. (S8) and (S11), and expanding, one finds

$$\mathcal{F}_{\rho(t)}^{\beta} = \underbrace{\operatorname{Tr}\left[\pi_{0}(\beta)\left(L_{\pi_{0}}^{\beta}\right)^{2}\right]}_{\mathcal{F}_{\pi_{0}}^{\beta}} + 2\int_{0}^{t} (\partial_{\beta}\lambda(s,\beta)) \operatorname{Tr}\left[\pi_{0}(\beta)L_{\pi_{0}}^{\beta}J_{V}(s)\right] ds + \underbrace{\int_{0}^{t} \int_{0}^{t} (\partial_{\beta}\lambda(s,\beta))(\partial_{\beta}\lambda(u,\beta))K(s,u,\beta) ds du}_{\mathcal{I}_{\beta}^{\beta}},$$
(S21)

with kernel

$$K(s, u, \beta) := \operatorname{Tr}[\pi_0(\beta) J_V(s) J_V(u)]. \tag{S22}$$

The mixed term vanishes,

$$\operatorname{Tr}\left[\pi_0(\beta)L_{\pi_0}^{\beta}J_V(s)\right] = 0,\tag{S23}$$

since $L_{\pi_0}^{\beta}$ and π_0 commute, while $J_V(s)$ is off-diagonal in their eigenbasis: their overall product is traceless. This leads directly to Eq. (1) of the main text, concluding our derivation of the decomposition $\mathcal{F}_{\rho(t)}^{\beta} = \mathcal{F}_{\pi_0}^{\beta} + \mathcal{I}_t^{\beta}$.

As a final note, since $(\partial_{\beta}\lambda(s,\beta))(\partial_{\beta}\lambda(u,\beta))$ is symmetric in (s,u), only the Hermitian (symmetric) part of the kernel contributes, namely

$$\int_{0}^{t} \int_{0}^{t} (\partial_{\beta} \lambda(s,\beta))(\partial_{\beta} \lambda(u,\beta)) K(s,u,\beta) ds du = \int_{0}^{t} \int_{0}^{t} (\partial_{\beta} \lambda(s,\beta))(\partial_{\beta} \lambda(u,\beta)) K_{S}(s,u,\beta) ds du,$$
 (S24)

where

$$K_S(s, u, \beta) := \frac{1}{2} \operatorname{Tr} \left[\pi_0(\beta) \left\{ J_V(s), J_V(u) \right\} \right] = \frac{1}{2} \left(K(s, u, \beta) + K(u, s, \beta) \right), \tag{S25}$$

while the antisymmetric part

$$K_A(s, u, \beta) := \frac{1}{2} \left(K(s, u, \beta) - K(u, s, \beta) \right)$$
(S26)

does not contribute, i.e.

$$\int_{0}^{t} \int_{0}^{t} (\partial_{\beta} \lambda(s,\beta))(\partial_{\beta} \lambda(u,\beta)) K_{A}(s,u,\beta) ds du = 0.$$
 (S27)

This yields Eq. (13) of the main text.

S2: SINGLE-SPIN PROBE

In this section, we discuss the results concerning the representative model of the driven spin probe. Our main goal is to instantiate Eq. (13) of the main text for a single spin- $\frac{1}{2}$ under coherent driving, showing explicitly the behaviour of the QFI increment at short and long times. Throughout we set, for clarity, $\hbar = k_{\rm B} = 1$.

We begin by computing the model-specific form of the increment \mathcal{I}_t^{β} from Eq. (S21). At t=0 the single spin is in a Gibbs state with respect to $H_0 = \frac{\Omega}{2}\sigma_z$ at inverse temperature β ,

$$\pi_0(\beta) = \frac{e^{-\beta H_0}}{Z_0} = \frac{1}{2} \left(\mathbb{1} - m \,\sigma_z \right), \qquad m = \tanh\left(\frac{\beta \Omega}{2}\right), \tag{S28}$$

with $Z_0 = \text{Tr}[e^{-\beta H_0}]$ and $\text{Tr}[\pi_0 \sigma_z] = -m$.

For t>0 we apply a transverse control $V=\sigma_x$ modulated by a cosinusoidal driving profile, $\lambda(t,\beta)=\lambda_0 G(\beta)\cos(\omega_{\rm d}t+\phi)$, so that

$$H(t,\beta) = H_0 + \lambda(t,\beta) V = \frac{1}{2} \mathbf{B}(t,\beta) \cdot \boldsymbol{\sigma}, \qquad \mathbf{B}(t,\beta) = (2\lambda_0 G(\beta) \cos(\omega_{\mathrm{d}} t + \phi), 0, \Omega), \tag{S29}$$

where $\sigma = (\sigma_x, \sigma_y, \sigma_z)$, λ_0 is the drive amplitude, $G(\beta)$ a Gaussian temperature envelope, and ω_d and ϕ the drive frequency and phase, respectively. We set, without loss of generality, $\phi = 0$. Since every SU(2) unitary acts as a proper rotation on spin operators, the Heisenberg-picture time-evolved perturbation can always be expressed as

$$V_H(t) = U_{t,\beta}^{\dagger} V U_{t,\beta} = \boldsymbol{\sigma} \cdot \mathbf{a}(t), \quad \mathbf{a}(0) = (1,0,0),$$
 (S30)

with the Bloch vector $\mathbf{a}(t) = (a_x(t), a_y(t), a_z(t))$ obeying the precession equation

$$\dot{\mathbf{a}}(t) = \mathbf{B}(t, \beta) \times \mathbf{a}(t). \tag{S31}$$

As discussed in the previous section, the information current operator is defined as

$$J_V(t) = -i \mathcal{J}_{\pi_0}^{-1} ([V_H(t), \pi_0]). \tag{S32}$$

Using Eq. (S28) and $[\sigma_i, \sigma_j] = 2i \epsilon_{ijk} \sigma_k$,

$$[\boldsymbol{\sigma} \cdot \mathbf{a}(t), \pi_0] = -\frac{m}{2} [\boldsymbol{\sigma} \cdot \mathbf{a}(t), \sigma_z] = i m (a_x(t)\sigma_y - a_y(t)\sigma_x).$$
 (S33)

Consider now a generic operator X that is fully off-diagonal in the eigenbasis of π_0 , and can thus be written as a linear combination of σ_x and σ_y . Using the integral representation of $\mathcal{J}_{\pi_0}^{-1}$ and Eq. (S28), we write

$$\mathcal{J}_{\pi_0}^{-1}(X) = 2\int_0^\infty e^{-s\pi_0} X e^{-s\pi_0} ds = 2\int_0^\infty e^{-s/2} e^{(sm/2)\sigma_z} X e^{-s/2} e^{(sm/2)\sigma_z} ds.$$
 (S34)

Since X is a linear combination of σ_x and σ_y , it anticommutes with σ_z , and one verifies that

$$e^{\alpha \sigma_z} X e^{\alpha \sigma_z} = X \qquad \forall \alpha \in \mathbb{R},$$
 (S35)

so that

$$e^{-s/2} e^{(sm/2)\sigma_z} X e^{-s/2} e^{(sm/2)\sigma_z} = e^{-s} X.$$
 (S36)

Therefore

$$\mathcal{J}_{\pi_0}^{-1}(X) = 2 \int_0^\infty e^{-s} \, ds \, X = 2X,\tag{S37}$$

and the overall information current takes the form

$$J_V(t) = 2m(a_x(t)\sigma_y - a_y(t)\sigma_x). \tag{S38}$$

To compute the integration kernel $K(s, u, \beta)$ and its symmetrized form, we exploit $\sigma_i \sigma_j = \delta_{ij} \mathbb{1} + i \epsilon_{ijk} \sigma_k$ to derive

$$J_V(s)J_V(u) = (2m)^2 \Big[(a_x(s)a_x(u) + a_y(s)a_y(u)) \mathbb{1} + i(a_x(s)a_y(u) - a_y(s)a_x(u))\sigma_z \Big].$$
 (S39)

In turn, given $Tr[\pi_0 \mathbb{1}] = 1$ and the definition of m,

$$K(s, u, \beta) = \text{Tr}[\pi_0 J_V(s)J_V(u)] = 4m^2 \Big[a_x(s)a_x(u) + a_y(s)a_y(u) - i m \left(a_x(s)a_y(u) - a_y(s)a_x(u) \right) \Big]. \tag{S40}$$

Finally, the symmetrized kernel, corresponding to the Hermitian part of $K(s, u, \beta)$, reads

$$K_S(s, u, \beta) = \frac{1}{2} \operatorname{Tr} \left[\pi_0 \{ J_V(s), J_V(u) \} \right] = 4m^2 \left[a_x(s) a_x(u) + a_y(s) a_y(u) \right]. \tag{S41}$$

We thus recover the exact, although in general involved, form of the increment at time t:

$$\mathcal{I}_t^{\beta} = \int_0^t \int_0^t \, \partial_{\beta} \lambda(s,\beta) \, \partial_{\beta} \lambda(u,\beta) \, 4m^2 [a_x(s)a_x(u) + a_y(s)a_y(u)] \, ds \, du. \tag{S42}$$

Short-time scaling

We now specialize to the short-time behaviour of Eq. (S42). To do so, we perform the standard reparametrization s = tz and u = tv, and expand the integrand in powers of the evolution time t.

For our driving protocol $\partial_{\beta}\lambda(t,\beta) = \lambda_0 G'(\beta)\cos(\omega_{\rm d}t) = \lambda_0 G'(\beta) + O(t^2)$, where $G'(\beta) = \partial_{\beta}G(\beta)$. From the precession equation $\dot{\mathbf{a}} = \mathbf{B} \times \mathbf{a}$ with $\mathbf{B}(0) = (2\lambda_0 G(\beta), 0, \Omega)$ and $\mathbf{a}(0) = (1, 0, 0)$, we obtain, to leading order in t,

$$a_x(t) = 1 + O(t^2), a_y(t) = \Omega t + O(t^2).$$
 (S43)

Hence, the symmetrized kernel admits the expansion

$$K_S(s, u, \beta) = 4m^2 [a_x(ts)a_x(tu) + a_y(ts)a_y(tu)] = 4m^2 [1 + \Omega^2 t^2 su + O(t^3)].$$
 (S44)

Substituting into

$$\mathcal{I}_{t}^{\beta} = t^{2} \int_{0}^{1} \int_{0}^{1} \partial_{\beta} \lambda(ts, \beta) \, \partial_{\beta} \lambda(tu, \beta) \, K_{S}(ts, tu, \beta) \, ds \, du$$
 (S45)

gives

$$\mathcal{I}_t^{\beta} = 4m^2 [\lambda_0 G'(\beta)]^2 t^2 + O(t^4), \tag{S46}$$

revealing the expected leading quadratic dependence on time, as is typical for unitary dynamics with analytic parameter dependence around t = 0.

Long-time scaling in the weak-field regime

To analyze the long-time behaviour of \mathcal{I}_t^{β} , we instead work under the weak-field assumption $\lambda_0 \ll \Omega$, which makes the precession equation analytically tractable. In this scenario, one can expand the Heisenberg-picture operator $V_H(t)$ around the interaction picture as

$$V_H(t) \approx V_I(t) - i \int_0^t \lambda(s, \beta) [V_I(s), V_I(t)] ds + O(\lambda_0^2), \tag{S47}$$

with $V_I(t) = e^{iH_0t}Ve^{-iH_0t} = \cos(\Omega t)\sigma_x - \sin(\Omega t)\sigma_y$ the interaction-picture evolved perturbation. Since $[V_I(s), V_I(t)] \propto \sigma_z$, the first-order correction vanishes when computing the commutator with $\pi_0(\beta)$ appearing in the information current. Then, up to first order in λ_0 , we obtain

$$J_V(t) = 2m(\cos(\Omega t)\,\sigma_y - \sin(\Omega t)\,\sigma_x) \ . \tag{S48}$$

In turn, the symmetrized kernel simplifies to

$$K_S(s, u, \beta) = 4 m^2 \cos(\Omega(s - u)), \qquad (S49)$$

having exploited the trigonometric identity $\cos(\Omega(s-u)) = \cos(\Omega s)\cos(\Omega u) + \sin(\Omega s)\sin(\Omega u)$.

Inserting Eq. (S49) into the definition of the increment and using $\partial_{\beta}\lambda(t,\beta) = \lambda_0 G'(\beta)\cos(\omega_{\rm d}t)$, we obtain to leading order in λ_0

$$\mathcal{I}_{t}^{\beta} = \int_{0}^{t} \int_{0}^{t} \partial_{\beta} \lambda(s, \beta) \, \partial_{\beta} \lambda(u, \beta) \, K_{S}(s, u, \beta) \, ds \, du \\
\approx 4m^{2} \left[\lambda_{0} G'(\beta) \right]^{2} \int_{0}^{t} \int_{0}^{t} \cos(\omega_{d} s) \cos(\omega_{d} u) \, \cos(\Omega(s - u)) \, ds \, du \, .$$
(S50)

Using once again the above-mentioned trigonometric identity, the double integral separates:

$$\mathcal{I}_{t}^{\beta} \approx 4m^{2} \left[\lambda_{0} G'(\beta)\right]^{2} \left[\left(\int_{0}^{t} \cos(\omega_{d} s) \cos(\Omega s) \, ds \right)^{2} + \left(\int_{0}^{t} \cos(\omega_{d} s) \sin(\Omega s) \, ds \right)^{2} \right]. \tag{S51}$$

Direct evaluation of each elementary integral gives

$$\mathcal{I}_t^{\beta} \approx 4m^2 \left[\lambda_0 G'(\beta)\right]^2 A(t), \tag{S52}$$

where

$$A(t) := \frac{\left(\omega_{\rm d}\sin(\omega_{\rm d}t)\cos(\Omega t) - \Omega\cos(\omega_{\rm d}t)\sin(\Omega t)\right)^2 + \left(\omega_{\rm d}\sin(\omega_{\rm d}t)\sin(\Omega t) + \Omega\cos(\omega_{\rm d}t)\cos(\Omega t) - \Omega\right)^2}{(\omega_{\rm d}^2 - \Omega^2)^2}.$$
 (S53)

In the resonance limit $\omega_d \to \Omega$, one finds

$$A(t) \to \frac{2\Omega^2 t^2 + 2\Omega t \sin(2\Omega t) - \cos(2\Omega t) + 1}{8\Omega^2}.$$
 (S54)

In the long-time limit, the oscillatory terms average out, so that the leading term remains proportional to t^2 . In particular, we obtain

$$\mathcal{I}_t^{\beta} \approx m^2 \big[\lambda_0 G'(\beta) \big]^2 t^2, \tag{S55}$$

which is of the form

$$\mathcal{I}_t^{\beta} \approx \left(\lambda_0 G'(\beta)\right)^2 \alpha(\beta) t^2, \tag{S56}$$

with $\alpha(\beta) = m^2$, as reported in Eq. (17) of the main text. This confirms that the quadratic scaling holds even at long times in the resonant, weak-field regime.